Barrier layer design reduces top electrode ion migration in perovskite solar cells

Saivineeth Penukula[1], Megh N Khanal[2], Mohin Sharma[3], Mritunjaya Parashar[3], Ross A. Kerner[4], Min Chen[4], Melissa A. Davis[4], Rafikul Ali Saha[5], Eduardo Solano[6], Maarten B.J. Roeffaers[5], Joseph J. Berry[4,7,8], Joseph M. Luther[4,8], Julian A. Steele[9,10], Axel Palmstrom[4], Vincent R Whiteside[2], Bibhudutta Rout[3], Ian R. Sellers[2], Nicholas Rolston[1]*

[1]Renewable Energy Materials and Devices Lab, School of Electrical, Computer and Energy Engineering (ECEE), Arizona State University, Tempe, Arizona 85281, USA

[2]Department of Electrical Engineering, 230 Davis Hall, University at Buffalo SUNY, Buffalo, New York 14260, USA

[3]Department of Physics, Ion Beam Laboratory, University of North Texas, Denton, Texas 76203, USA

[4]National Renewable Energy Laboratory, Golden, Colorado 80309, USA

[5]cMACS, Department of Microbial and Molecular Systems, KU Leuven, Celestijnenlaan 200F, 3001 Heverlee, Belgium

[6]NCD-SWEET Beamline, ALBA Synchrotron Light Source, 08290 Cerdanyola del Vallès, Barcelona, Spain

[7]Department of Physics, University of Colorado Boulder, Boulder, Colorado 80309, USA

[8]Renewable and Sustainable Energy Institute, University of Colorado Boulder, Boulder, Colorado 80309, USA

[9]Australian Institute of Bioengineering and Nanotechnology, The University of Queensland, St Lucia, QLD 4072, Australia

[10]School of Mathematics and Physics, The University of Queensland, Brisbane, QLD 4072, Australia

*Corresponding author and lead contact:

Prof. Nicholas Rolston

Renewable Energy Materials and Devices Lab,

School of Electrical, Computer, and Energy Engineering (ECEE),

Arizona State University,

Tempe, AZ, USA

e-mail: nicholas.rolston@asu.edu

ORCID: orcid.org/0000-0001-8093-1689

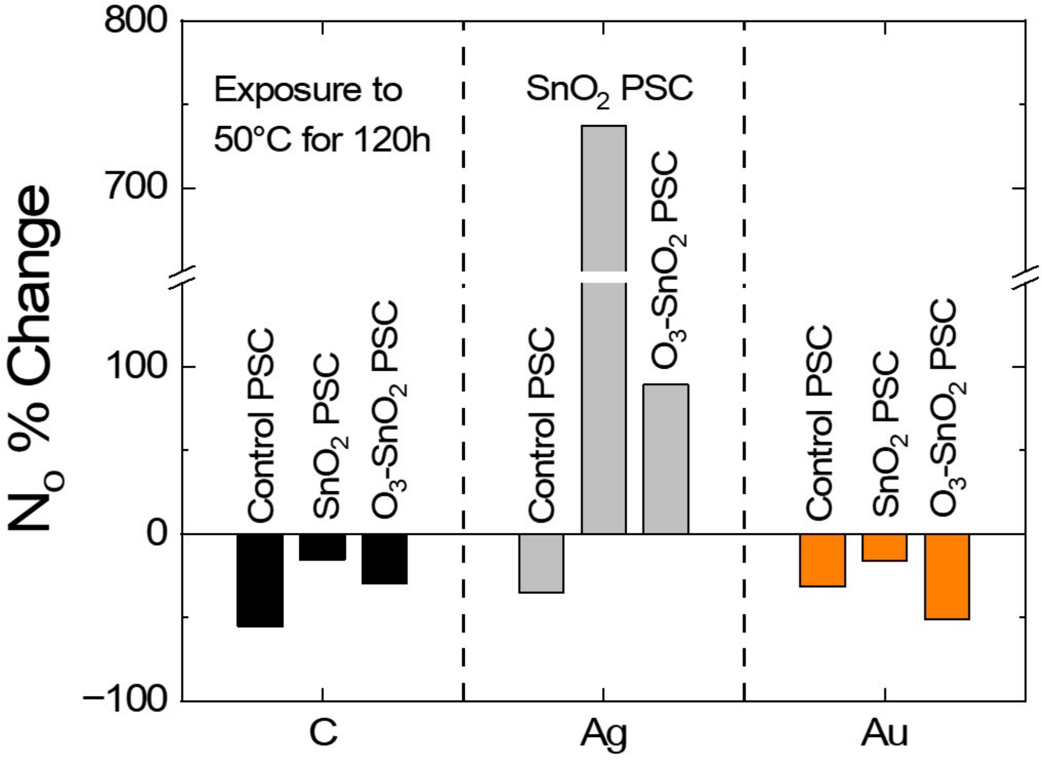

Fig. S1 Percentage change in N_o for control PSC, SnO_2 PSC, and O_3-SnO_2 PSC with C, Ag, and Au top electrodes after exposure of the PSCs to 50°C for 120h

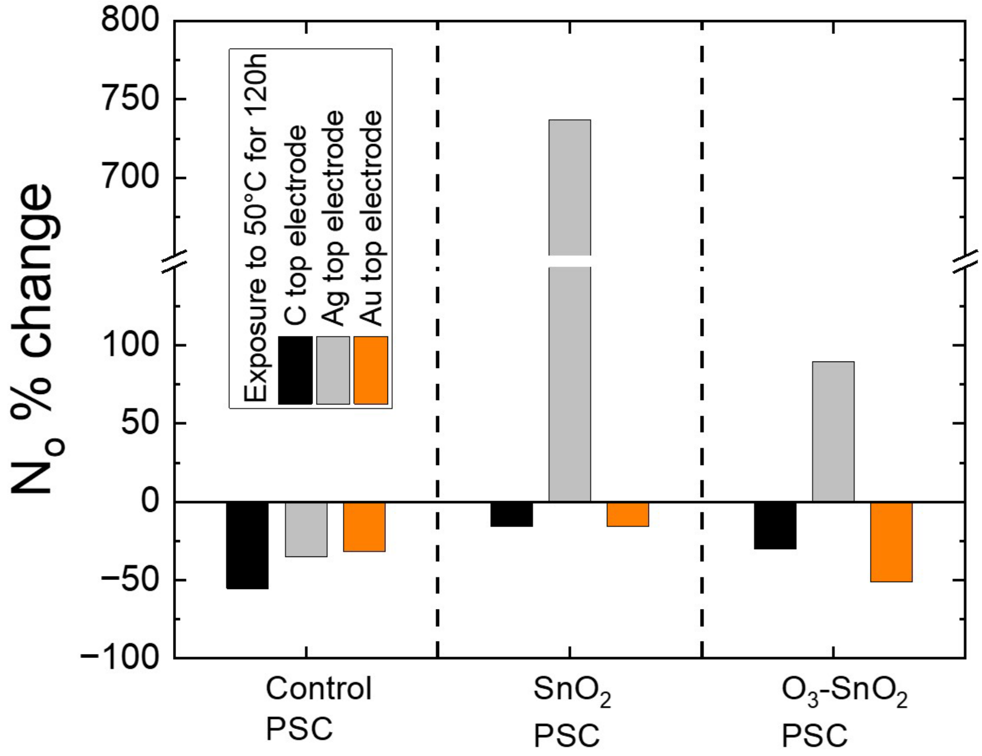

Fig. S2 Percentage change in N_o for control PSC, SnO_2 PSC, and O_3-SnO_2 PSC with C, Ag, and Au top electrodes after exposure of the PSCs to 50°C for 120h

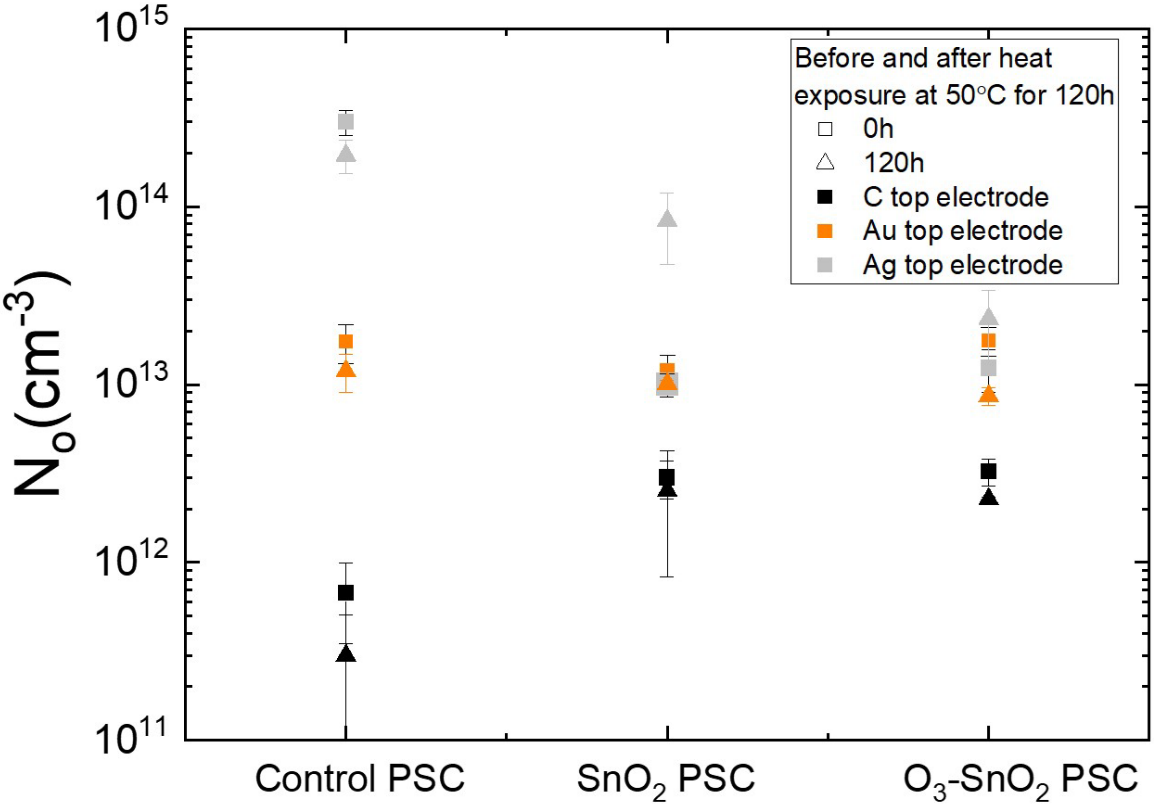

Fig. S3 N_o for control PSC, SnO_2 PSC, and O_3-SnO_2 PSC with C, Ag, and Au top electrodes before and after exposure of the PSCs to 50°C for 120h

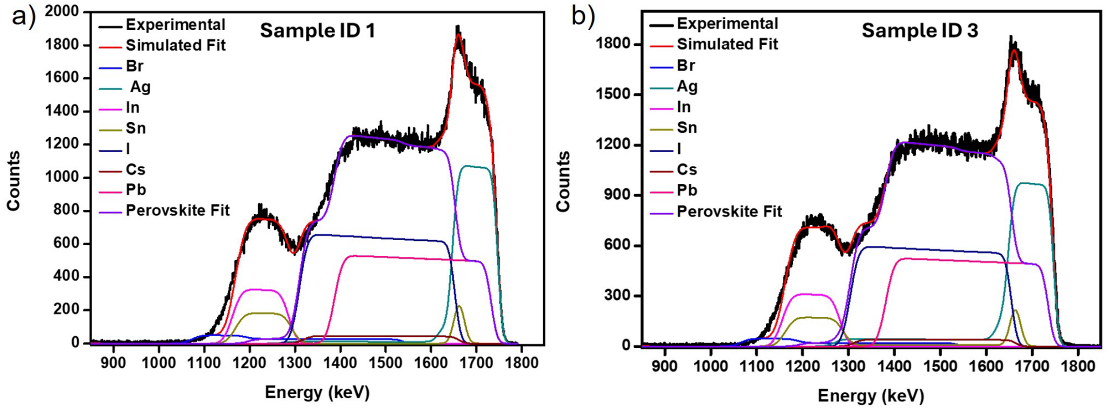

Fig. S4 Unaged vs aged RBS spectrum of control PSCs with the experimental spectrum and SIMNRA simulation fits a) unaged control PSC b) aged control PSC

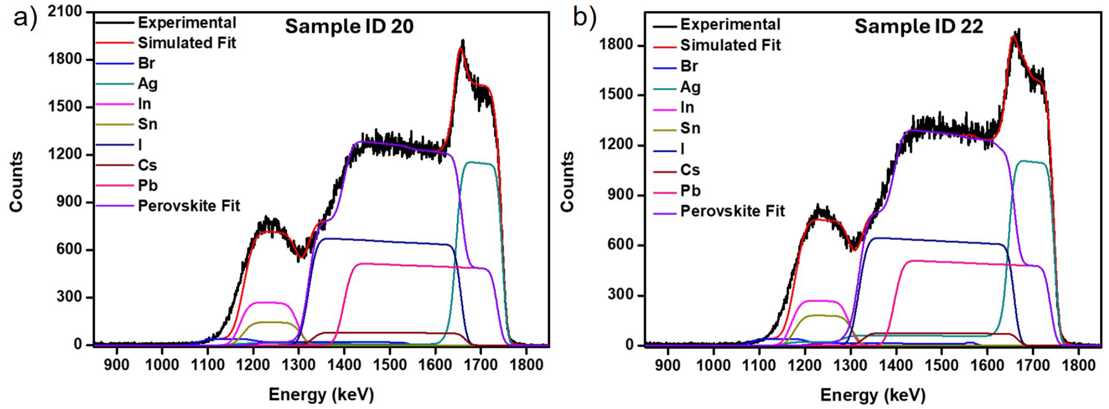

Fig. S5 Unaged vs aged RBS spectrum of SnO_2 PSCs with the experimental spectrum and SIMNRA simulation fits a) unaged control PSC b) aged SnO_2 PSC

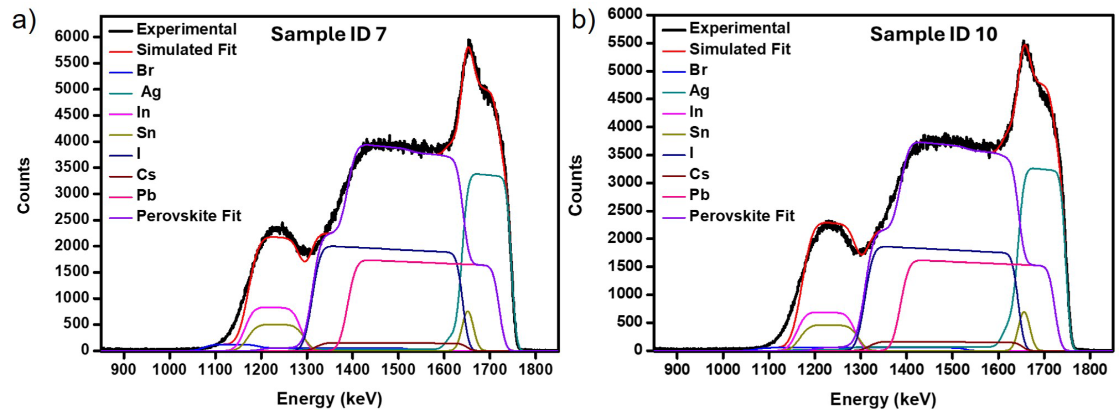

Fig. S6 Unaged vs aged RBS spectrum of O_3-SnO_2 PSCs with the experimental spectrum and SIMNRA simulation fits a) unaged control PSC b) aged O_3-SnO_2 PSC

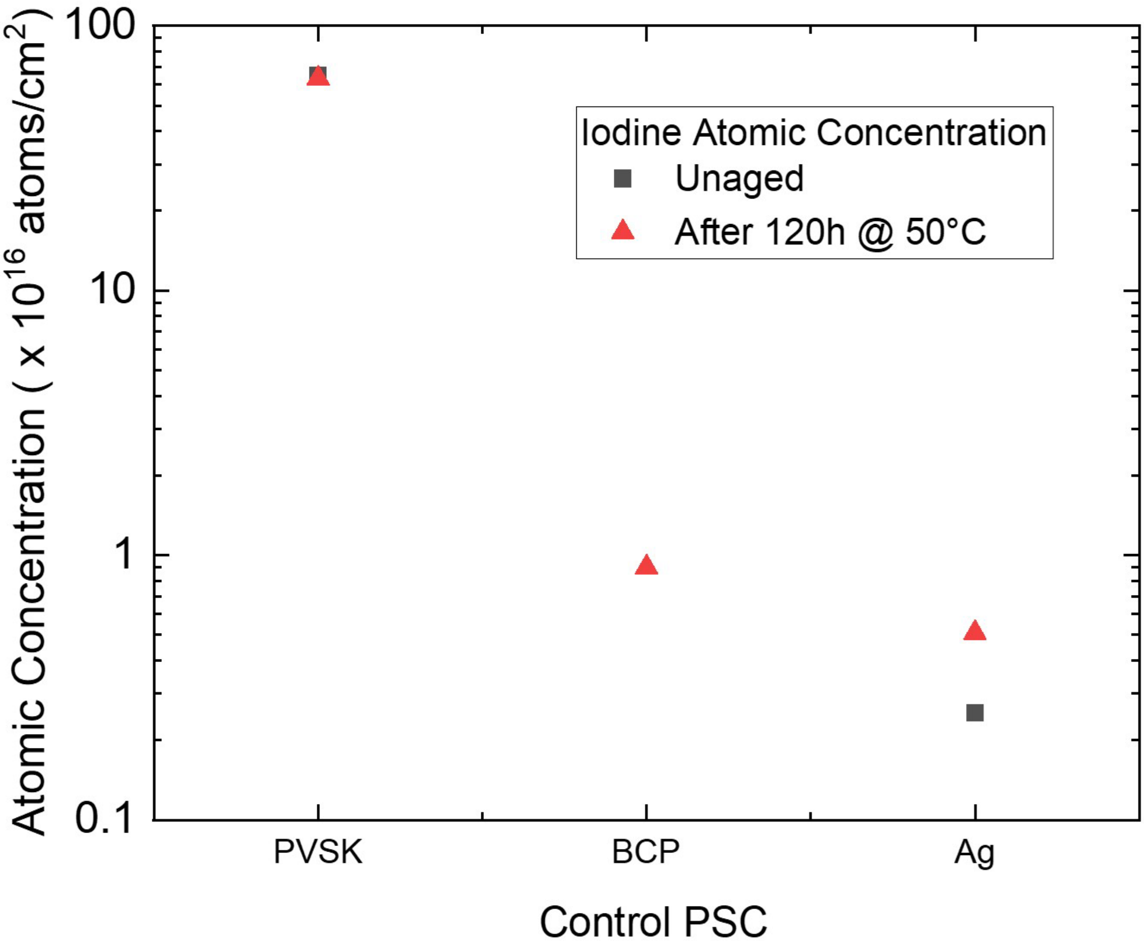

Fig. S7 Unaged vs aged atomic concentration of iodine (I) as determined using RBS in the MHP layer, BCP layer, and Ag layer for control PSC.

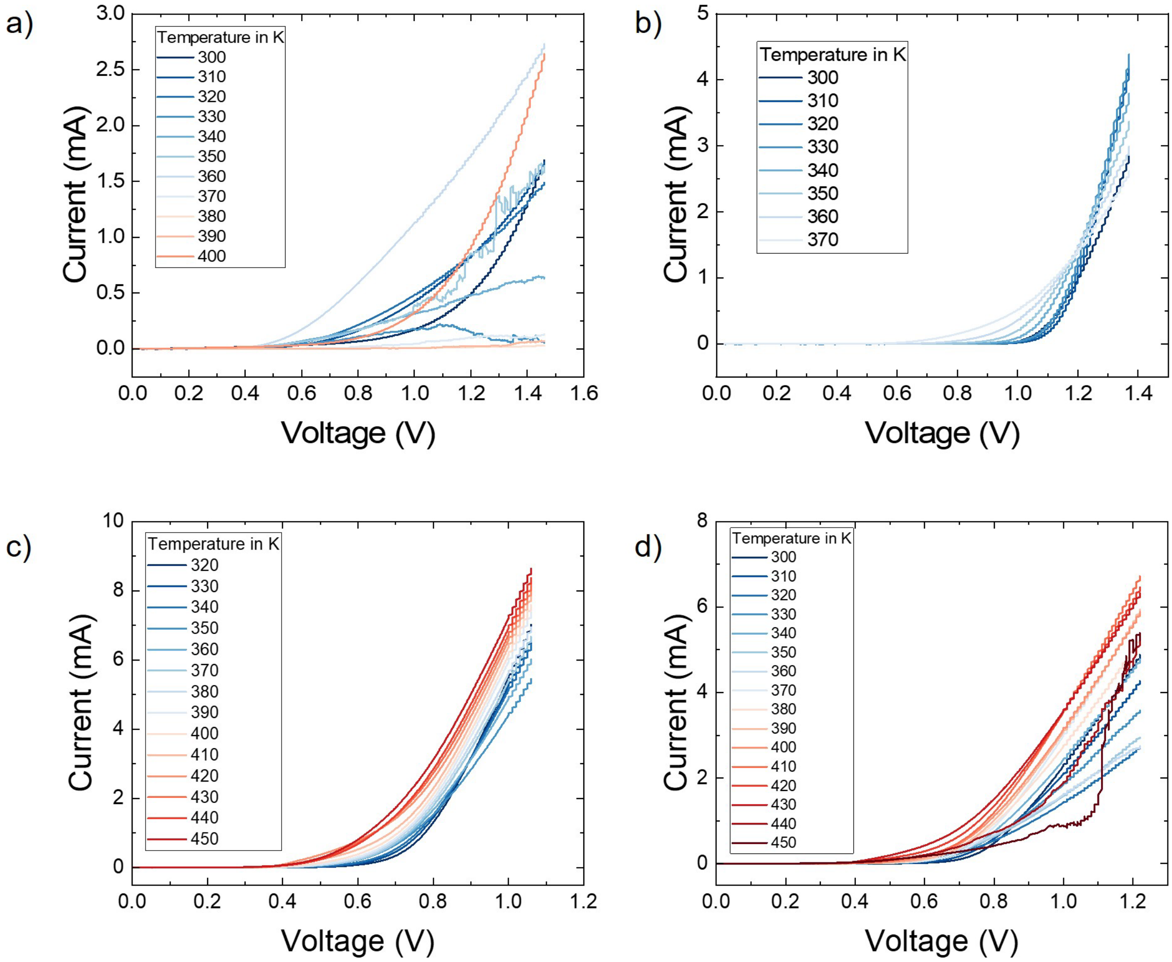

Fig. S8 Dark IV response over temperature sweep from 300K to 450K of (a) Control PSC, (b) SAM-based PSC, (c) SnO_2 PSC, and (d) O_3- SnO_2 PSC

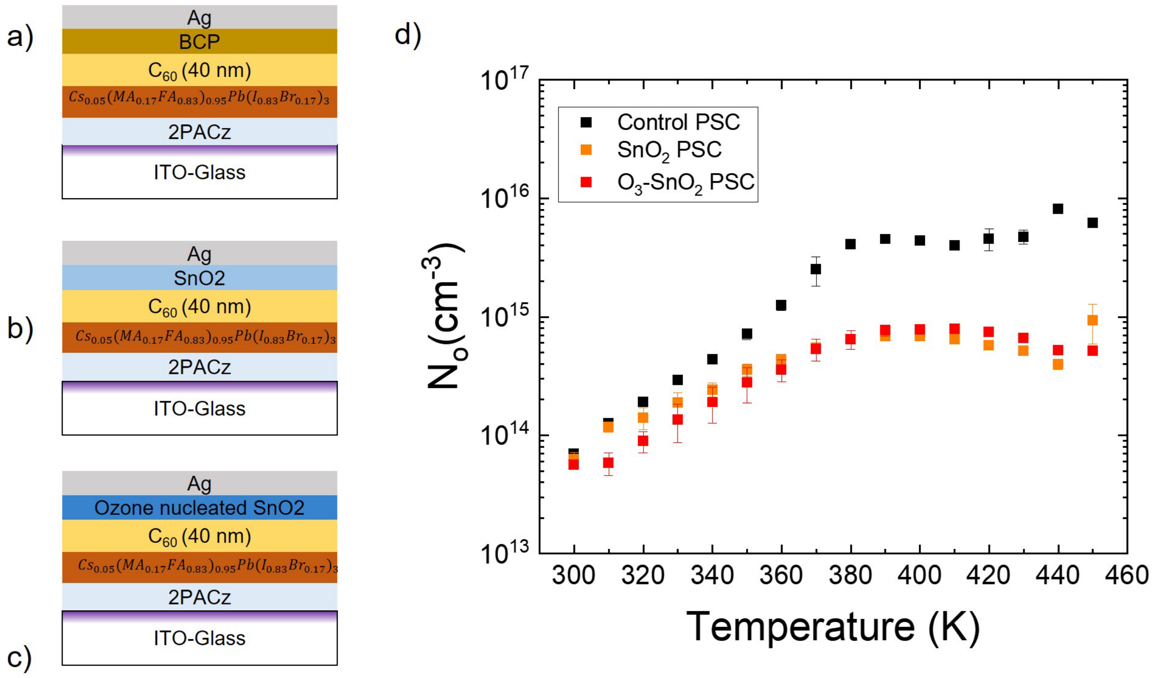

Fig. S9 (a-c) Device stack structures used for the performance measurements (a) Control PSC, (b) SnO_2 PSC, (c) O_3-SnO_2 PSC, and (d) N_o of PSCs versus temperature.

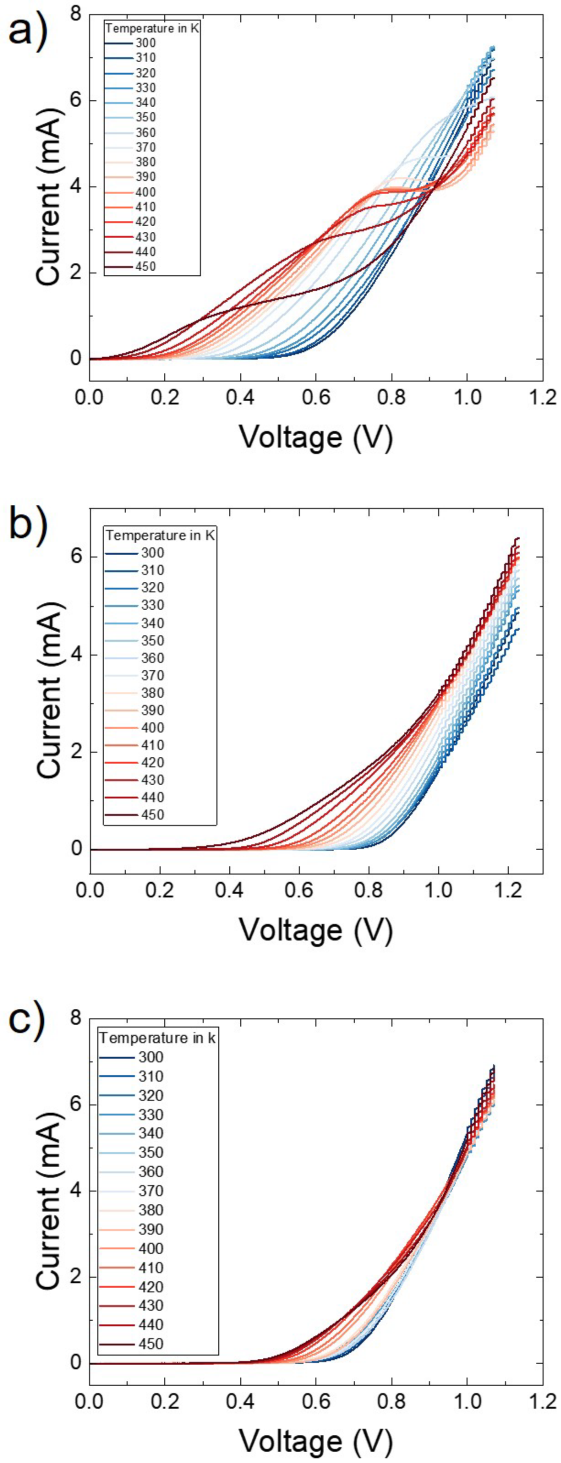

Fig. S10 Dark IV response over temperature sweep from 300K to 450K of (a) Control PSC, (b) SnO_2 PSC, and (c) O_3- SnO_2 PSC

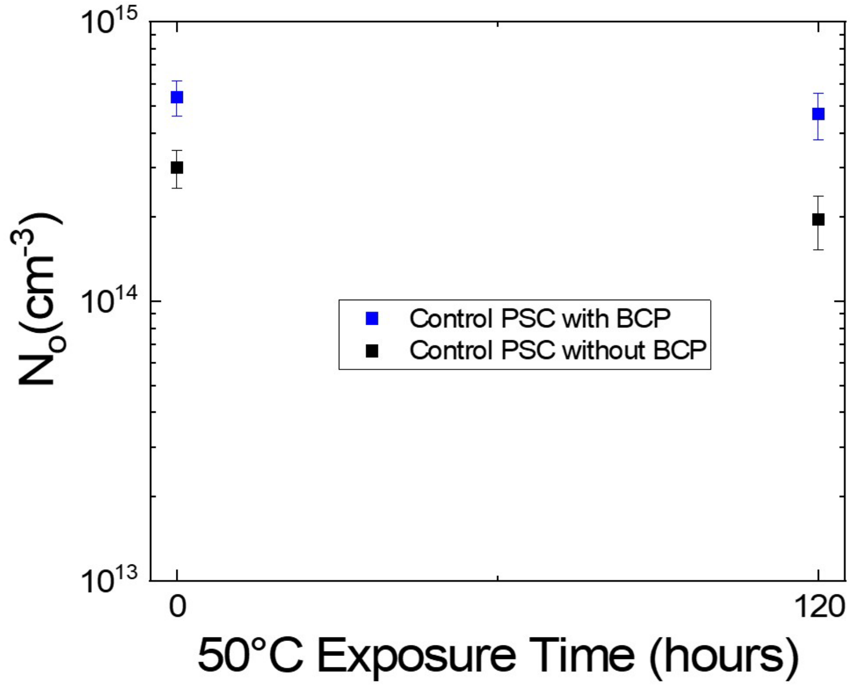

Fig. S11 N_o vs time for control PSC with and without BCP layer after being exposed to a heat of 50°C for 120 hours.

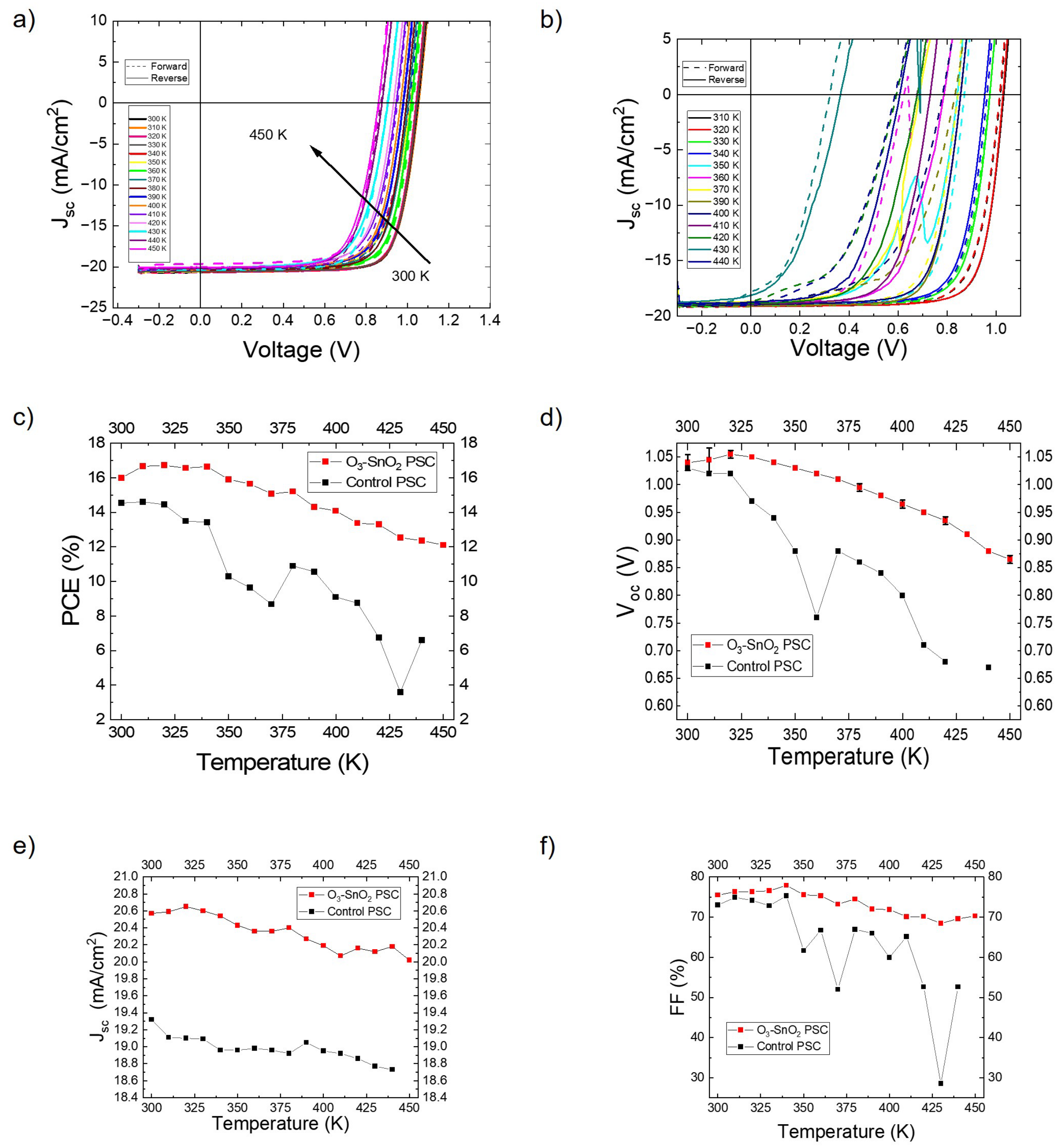

Fig. S12 Temperature-dependent responses of PSCs in the range of 300K to 450K. (a) Light JV response of O_3-SnO_2 PSC, (b) Light JV response of control PSC. O_3-SnO_2 PSC vs control PSC (c) PCE, (d) V_{OC}, (e) J_{SC}, (f) FF.

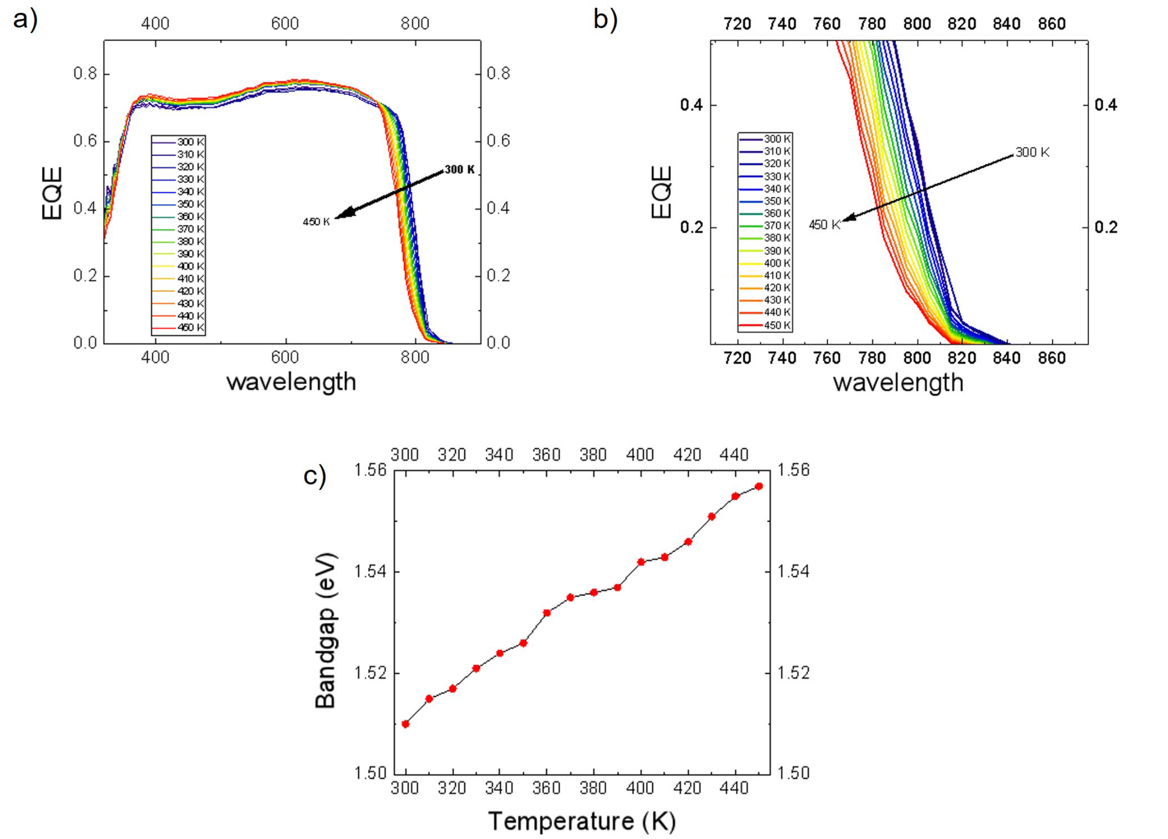

Fig. S13 Temperature-dependent responses of O_3-SnO_2 PSC in the range of 300K to 450K. (a) EQE, (b) EQE zoomed in, (c) Bandgap.

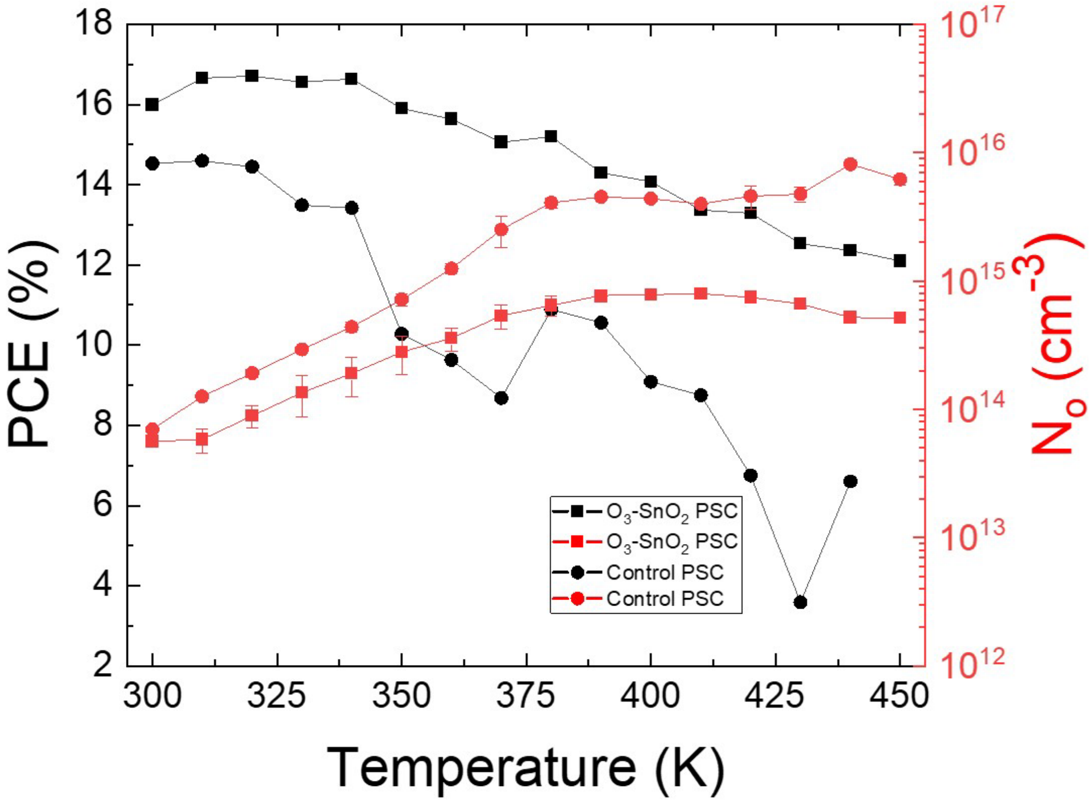

Fig. S14 N_o vs PCE of O_3-SnO_2 and control PSC in the range of 300K – 450K.

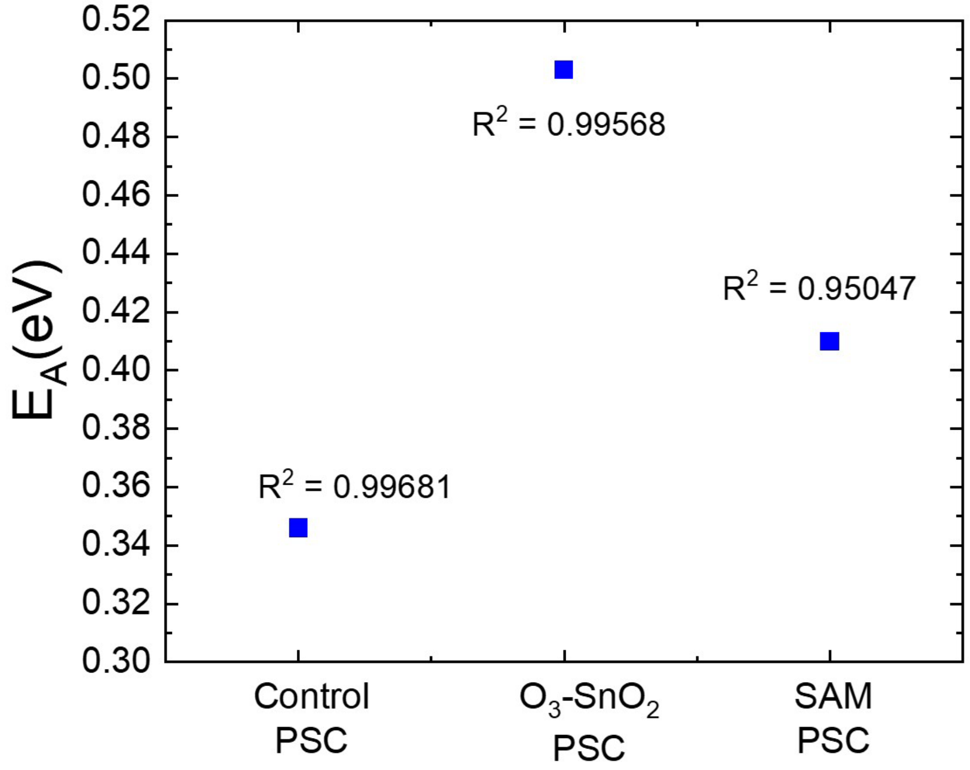

Fig. S15 Activation energy (E_A) with R^2 values of (a) Control PSC, (b) O_3-SnO_2 PSC, and (c) SAM-based PSC.

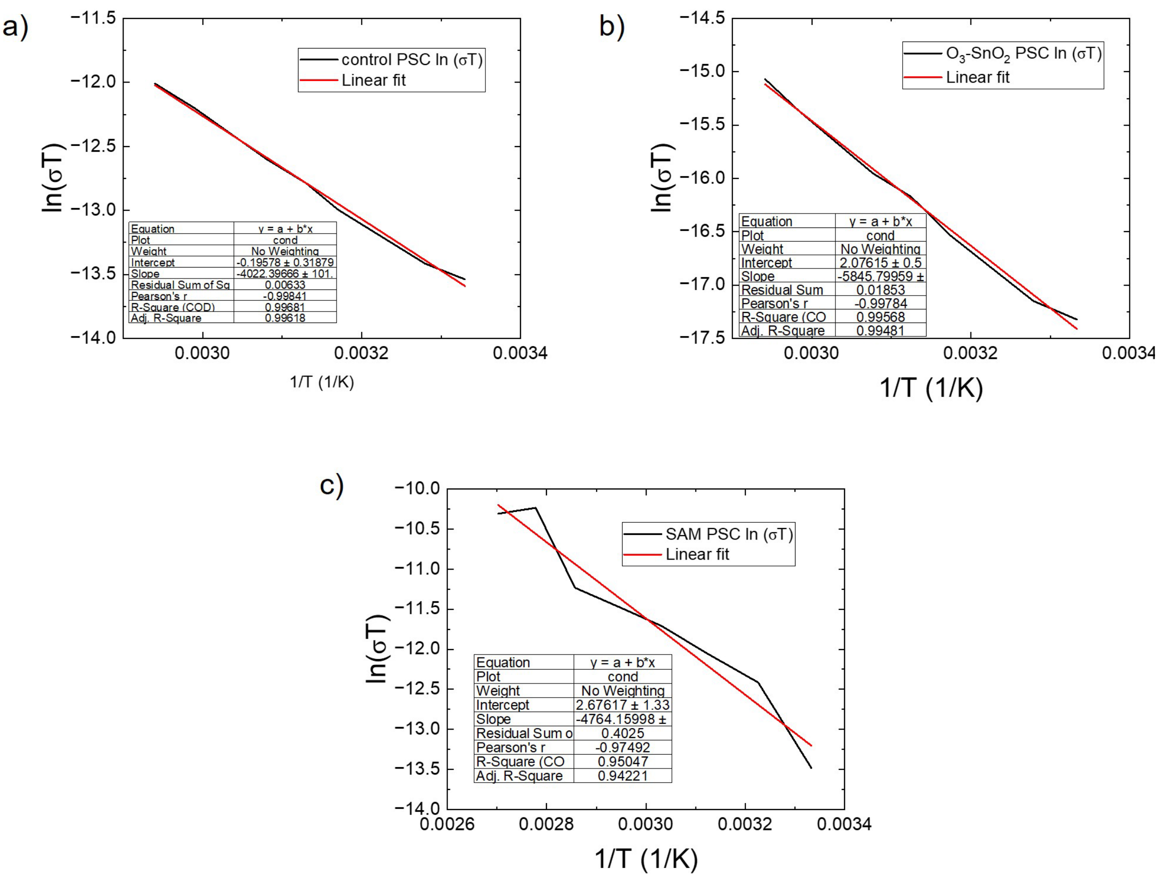

Fig. S16 Activation energy fits of (a) Control PSC, (b) O_3-SnO_2 PSC, and (c) SAM-based PSC

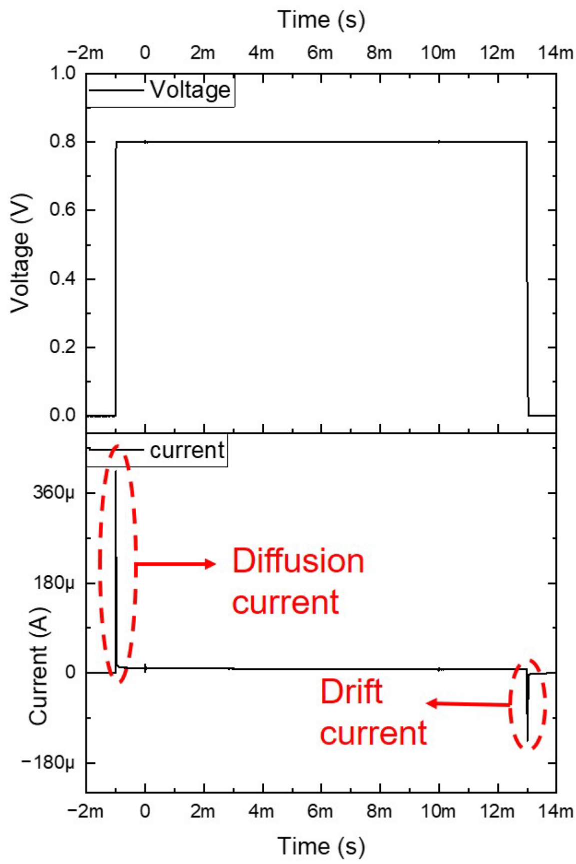

Fig. S17 Transient dark current measurement (TDC) showing the applied voltage to the device and the transient current response recorded with isolated peaks of diffusion current and drift current.

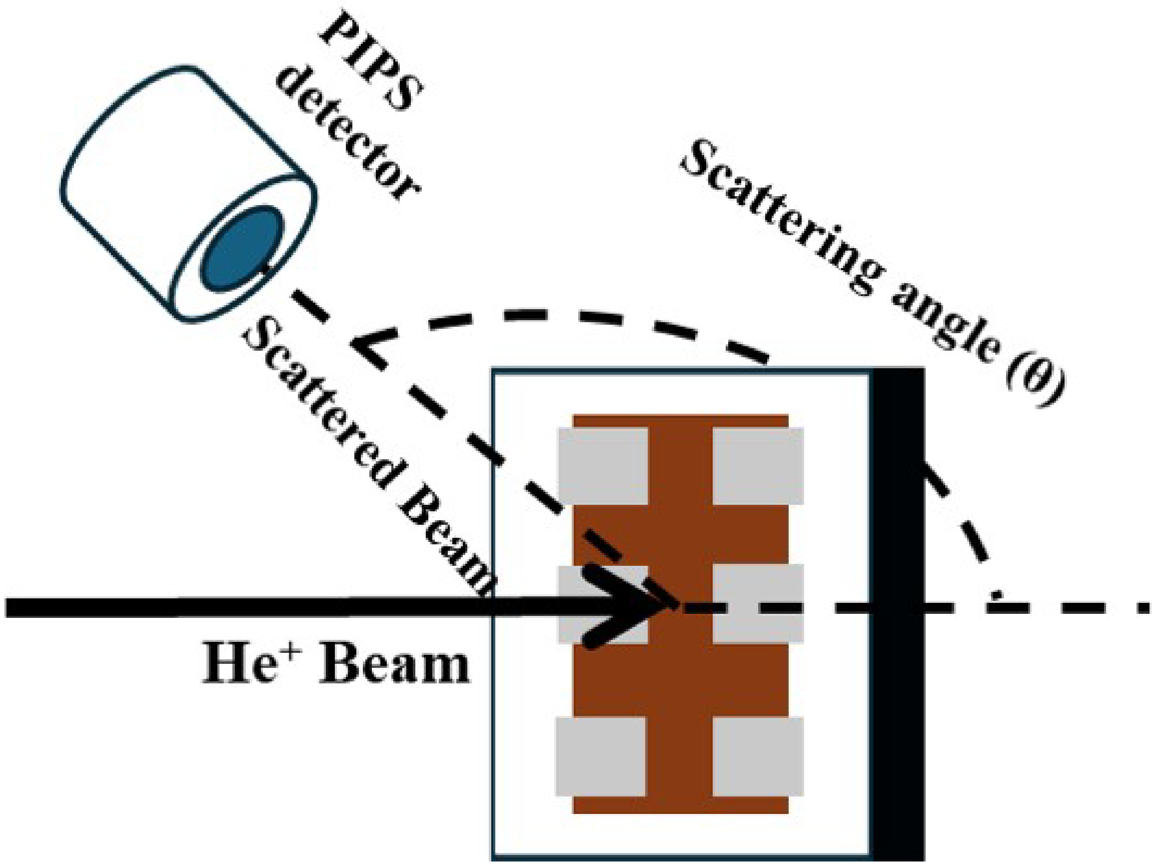

Fig. S18 Schematic of Rutherford Backscattering Spectroscopy (RBS) setup for target characterization

Layer-1 Ag electrode ($\times10^{15}$ atoms/cm^2)	layer-2 BCP ($\times10^{15}$ atoms/cm^2)	Layer-3 C_{60} ($\times10^{15}$ atoms/cm^2)	Layer-4 Perovskite ($\times10^{15}$ atoms/cm^2)	Layer-5 2-PACz ($\times10^{15}$atoms/cm^2)	Layer-6 ITO ($\times10^{15}$atoms/cm^2)
513.75	159.09	255.73	2646.84	14.39	989.52
O	H	C	H	H	O
15.49	66.33	248.69	550.97	2.18	703.17
Ag	C	Ag	C	C	Br
495.72	85.85	7.04	403.38	1.73	30.08
I	N		N	N	Ag
2.54	6.91		451.96	0.22	5.15
			O	P	In
			251.08	0.20	105.71
			Br	I	Sn
			44.63	10.07	54.93
			Ag		I
			10.05		90.46
			I		
			650.96		
			Cs		
			72.93		
			Pb		
			210.88		

Table S1 Atomic concentrations of unaged control PSC as determined using RBS

Layer-1 Ag electrode ($\times10^{15}$ atoms/cm^2)	layer-2 BCP ($\times10^{15}$ atoms/cm^2)	Layer-3 C_{60} ($\times10^{15}$ atoms/cm^2)	Layer-4 Perovskite ($\times10^{15}$ atoms/cm^2)	Layer-5 2-PACz ($\times10^{15}$atoms/cm^2)	Layer-6 ITO ($\times10^{15}$atoms/cm^2)
538.53	63.36	261.55	2729.91	4.49	957.25
O	H	C	H	H	O
61.32	20.96	251.51	652.33	2.22	653.59
Ag	C	Ag	C	C	Br
472.11	27.08	10.04	353.75	1.75	30.29
I	N		N	N	Ag
5.10	2.26		451.85	0.25	9.11
	Br		O	P	In
	4.02		251.67	0.28	105.53
	I		Br		Sn
	9.04		30.28		68.28
			Ag		I
			75.21		90.45
			I		
			633.81		
			Cs		
			69.65		
			Pb		
			211.37		

Table S2 Atomic concentrations of control PSC after aging at 50°C for 120h as determined using RBS

Layer-1 Ag electrode ($\times 10^{15}$ atoms/cm^2)	layer-2 SnO_2 ($\times 10^{15}$ atoms/cm^2)	Layer-3 C_{60} ($\times 10^{15}$ atoms/cm^2)	Layer-4 Perovskite ($\times 10^{15}$ atoms/cm^2)	Layer-5 2-PACz ($\times 10^{15}$atoms/cm^2)	Layer-6 ITO ($\times 10^{15}$atoms/cm^2)
531.49	112.32	258.44	2751.43	13.42	913.21
O	O	C	H	H	O
58.66	87.20	249.35	655.67	2.21	599.10
Ag	Sn	Ag	C	C	Br
472.83	25.13	9.09	355.31	1.69	38.05
			N	N	Ag
			451.00	0.23	0.00
			O	P	In
			259.59	0.22	130.25
			Br	I	Sn
			63.30	9.08	70.71
			Ag		I
			14.54		75.10
			I		
			677.84		
			Cs		
			42.55		
			Pb		
			231.64		

Table S3 Atomic concentrations of unaged SnO_2 PSC as determined using RBS

Layer-1 Ag electrode ($\times 10^{15}$ atoms/cm^2)	layer-2 SnO_2 ($\times 10^{15}$ atoms/cm^2)	Layer-3 C_{60} ($\times 10^{15}$ atoms/cm^2)	Layer-4 Perovskite ($\times 10^{15}$ atoms/cm^2)	Layer-5 2-PACz ($\times 10^{15}$atoms/cm^2)	Layer-6 ITO ($\times 10^{15}$atoms/cm^2)
559.65	123.30	230.13	2858.95	9.34	920.05
O	O	C	H	H	O
120.07	86.07	220.10	752.48	2.08	600.26
Ag	Ag	Ag	C	C	Br
439.58	12.08	10.04	351.06	1.58	37.71
	Sn		N	N	Ag
	25.14		347.34	0.46	0.00
			O	P	In
			348.87	0.19	131.35
			Br	I	Sn
			49.08	5.04	70.32
			Ag		I
			60.12		75.39
			Sn		Pb
			10.01		5.01
			I		
			653.52		
			Cs		
			42.06		
			Pb		
			244.42		

Table S4 Atomic concentrations of SnO_2 PSC after aging at 50°C for 120h as determined using RBS

Layer-1 Ag electrode ($\times 10^{15}$ atoms/cm^2)	layer-2 SnO_2_O_3 ($\times 10^{15}$ atoms/cm^2)	Layer-3 C_{60} ($\times 10^{15}$ atoms/cm^2)	Layer-4 Perovskite ($\times 10^{15}$ atoms/cm^2)	Layer-5 2-PACz ($\times 10^{15}$atoms/cm^2)	Layer-6 ITO ($\times 10^{15}$atoms/cm^2)
577.15	165.25	243.00	2822.00	16.89	958.00
O	O	C	H	H	O
70.00	132.25	235.00	790.00	2.14	677.00
Ag	Ag	Ag	C	C	Br
507.15	5.00	8.00	400.00	1.68	30.00
	Sn		N	N	In
	28.00		430.00	0.17	104.98
			O	P	Sn
			250.00	0.15	61.02
			Br	I	I
			40.00	12.75	85.00
			Ag		
			12.00		
			I		
			625.00		
			Cs		
			45.00		
			Pb		
			230.00		

Table S5 Atomic concentrations of unaged O_3-SnO_2 PSC as determined using RBS

Layer-1 Ag electrode ($\times 10^{15}$ atoms/cm^2)	layer-2 SnO_2_O_3 ($\times 10^{15}$ atoms/cm^2)	Layer-3 C_{60} ($\times 10^{15}$ atoms/cm^2)	Layer-4 Perovskite ($\times 10^{15}$ atoms/cm^2)	Layer-5 2-PACz ($\times 10^{15}$atoms/cm^2)	Layer-6 ITO ($\times 10^{15}$atoms/cm^2)
529.03	148.04	260.34	2659.50	4.36	1081.31
O	O	C	H	H	O
31.87	110.60	248.27	553.02	2.19	780.25
Ag	Ag	Ag	C	C	Br
497.16	10.05	12.07	402.19	1.74	15.08
	Sn		N	N	In
	27.38		452.47	0.22	95.51
			O	P	Sn
			251.37	0.20	61.36
			Br		I
			45.25		126.01
			Ag		Ag
			30.16		3.11
			I		
			628.43		
			Cs		
			65.36		
			Pb		
			231.26		

Table S6 Atomic concentrations of O_3-SnO_2 PSC after aging at 50°C for 120h as determined using RBS

Device	Unaged	Aged
Control PSC 0.3° (top surface)	1.846	0.233
Control PSC 5° (Bulk)	Inf	0.214
SnO_2 PSC 0.3° (top surface)	3.228	1.877
SnO_2 PSC 5° (Bulk)	Inf	Inf
O_3-SnO_2 PSC 0.3° (top surface)	6.53	5.37
O_3-SnO_2 PSC 5° (Bulk)	Inf	Inf

Table S7 Integrated peak area ratio between PVSK (110) and degradation product for unaged PSCs vs PSCs subjected to 50°C for 120h.

Supplementary Note 1

For RBS analysis using SIMNRA and MultiSIMNRA programs, the layer's structure or thickness is usually expressed as aerial density (atoms/cm²). Then to begin with, the known thicknesses of the individual layers are entered to simulate the spectrum. The simulated spectrum is then compared with the experimental spectrum and then changes in the layer and elemental composition are made accordingly to best fit the simulated curve to the experimental curve. Once the best fit is achieved, the information for the individual layers is extracted. To determine the goodness of the fit and uncertainty of the fitted curve, Reduced chi-square (χ_r^2) value was obtained from the SIMNRA program. Reduced chi-square (χ_r^2) is defined as the $\chi_r^2 = \frac{\chi^2}{N}$. Where χ^2 represents the quadratic deviation between experimental and simulated data for the desired regions and N is the number of channels. The channels are calibrated to the backscattered helium ion energy. The χ_r^2 value between 2 and 5 suggests a satisfactory agreement between the experimental data and the simulation.[1,2] The χ_r^2 values are determined within the 1357 - 1820 keV energy range. The χ_r^2 values for sample ID 20 and 22 are 2.42 and 2.41 respectively, and for sample ID 1 and 3 are 2.04 and 2.58 respectively, also for sample ID 7,13 are 2.95 and 3.03 respectively.

Sensitivity analysis was performed on sample ID 22 by manually changing the concentration of Ag in layer 4 and then simulating the fits. This analysis has shown that any change in the Ag concentration from the best-fit value (with χ_r^2 value of 2.41) is leading to a drastic increase in the χ_r^2 value and hence affecting the goodness of the fit.

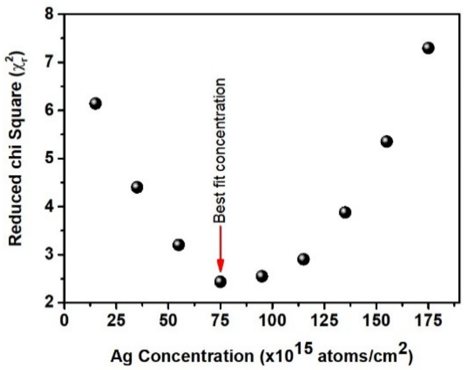

References

[1] Matej Mayer, **1997**.

[2] T. F. Silva, C. L. Rodrigues, M. Mayer, M. V Moro, G. F. Trindade, F. R. Aguirre, N. Added, M. A. Rizzutto, M. H. Tabacniks, *Nucl Instrum Methods Phys Res B* **2016**, *371*, 86.